

Architectural and Immunohistochemical Characterization of Biliary Ductules in Normal Human Liver

Katalin Dezső, Sándor Paku, Veronika Papp, Eszter Turányi, and Peter Nagy

The canals of Hering or biliary ductules have been described to connect the bile canaliculi with the interlobular bile ducts, and thus forming the distal part of the biliary tree. Studies in the last two decades suggested that the cells constructing these ductules could behave as hepatic progenitor cells. The canals of Hering are confined to the periportal space in the rat, while they have been reported to spread beyond the limiting plate in human liver. The distribution of the distal biliary ductules in normal human hepatic tissue has been investigated in our recent experiments. We could demonstrate the presence of interlobular connective tissue septa in a rudimentary form in healthy livers. The canals of Hering run in these septa in line with the terminal branches of the portal vein and hepatic arteries. This arrangement develops in the postnatal period but regresses after early childhood. The canals of Hering can be identified by the unique epithelial membrane antigen (EMA)⁻/CD56⁺/CD133⁺ immunophenotype. The canals of Hering leave the periportal space and spread into the liver parenchyma along rudimentary interlobular septa outlining the hepatic lobules. Our observations refine the original architectural description of the intraparenchymal portion of the canals of Hering in the human liver. The distinct immunophenotype supports their unique biological function.

Introduction

1 THE EXISTENCE OF A progenitor cell population in the liver
2 has become generally accepted [1,2], and the clinical
3 application of these cells have been of tremendous interest
4 [3,4]. Today, liver transplantation is the only available cura-
5 tive treatment for liver failure, either in cirrhosis or in fulmi-
6 nant liver necrosis. However, the number of available donor
7 livers sets the limit for the application of this procedure and
8 alternative treatments are being sought. Transdifferentiation
9 of bone marrow cells into hepatocytes does not seem to be
10 efficient enough for clinical application [5–7]. Conversely,
11 efficient hepatic regeneration has been recorded from the
12 endogenous liver progenitor cells in human [8,9].

13 Most data refer to the canals of Hering as the site of the
14 hepatic progenitor cell compartment [1,2,10]. This structure
15 was described by Hering as “hepatic capillaries” [11], which
16 maintained the link between bile ducts and the hepato-
17 cyte canalicular system. Later, it had been proposed to be
18 the niche for hepatic progenitor cells [12,13]. The niche is a
19 special microenvironment, which has a major impact on
20 the maintenance and activation of the stem/progenitor cell
21 compartment [14]. Therefore, the exact identification and

characterization of this structure is necessary to understand 22
its behavior under normal and pathological conditions. 23

24 The canals of Hering are usually shown as short, straight
25 ductules at the border of the periportal connective tissue and
26 liver parenchyma, but probably this conformation is oversim-
27 plified. We have recently characterized the hepatic progenitor
28 cell niche in rat liver by laser scanning confocal microscopy
29 [15]. Long, branching ductules have been observed, strictly
30 inside the periportal connective tissue. They had contact with
31 the bile canalicular system at the limiting plate. Their unique
32 CK19⁺/CK7⁻ immunophenotype has made their identifi-
33 cation within the biliary tree easier. However, no CK7⁻ bili-
34 ary structures could be observed in human liver specimens.
35 Furthermore, the canals of Hering have been described to
36 spread into the hepatic lobule in the normal human liver [16].
37 These observations suggest that the organization of the canals
38 of Hering in human liver is different from the traditional sim-
39 ple view as well as from the architecture we saw in rat liver.

40 In our present study, we set out to collect normal human
41 liver tissue from individuals of various ages and analyzed
42 the architecture and immunophenotype of the biliary
43 ductules by confocal microscopy.

First Department of Pathology and Experimental Cancer Research, Semmelweis University, Budapest, Hungary.

Materials and Methods

44 Normal human liver specimens were collected from
45 cadavers of spontaneous premature birth neonates with-
46 out developmental abnormalities and individuals who died
47 suddenly in accidents without morphological signs and
48 anamnestic data of any liver disease. (Age and gender of the
49 patients: 3 males, 23rd week of pregnancy; 4 females, 23rd
50 week of pregnancy; 1 male, 39th week of pregnancy; 2 males,
51 3 years; 1 female, 3 years; 1 female, 13 years; 1 male, 20 years;
52 1 male, 26 years old.) All autopsies were performed within
53 24 h following death. The liver samples were thoroughly
54 examined on formalin-fixed, paraffin-embedded liver sec-
55 tions with H&E, diastase PAS, Prussian blue, orcein and
56 Masson's trichrome stainings; no fibrosis, ductular reaction,
57 or other pathological alterations were observed. Snap frozen
58 liver samples were stored at -80°C .

59 Frozen sections (10–20 μm) were fixed in methanol and
60 were incubated at room temperature (1 h) with a mixture of
61 primary antibodies (Supplementary Table 1), (Supplementary
62 materials are available online at <http://www.liebertpub.com/>)
63 followed by the appropriate fluorescent secondary antibodies
64 (Jackson ImmunoResearch, West Grove, PA). All samples were
65 analyzed by confocal laser scanning microscopy using Bio-
66 Rad MRC-1024 system (Bio-Rad, Richmond CA).

67 The procedure has been approved by the ethical commit-
68 tee of Semmelweis University.

69 Quantitative analysis of immunohistochemical staining

70 The livers of two 3-year-old children and the 20-, 26-year-
71 old adults were used for quantitation. Consecutive frozen
72 sections were co-stained for CK7/EMA, CK7/CD56, and CK7/
73 CD133. The number of CK7-stained structures was deter-
74 mined. The double-stained structures were counted and the
75 results were given as percent of the CK7+ structures.

Results

Distribution of hepatic ductules in the liver parenchyma

76 When sections from the livers of 3-year-old healthy chil-
77 dren were stained for panCK, CK7, and laminin, hepatic
78 ductules surrounded by basement membrane could be
79 observed in the parenchyma far from the portal spaces
80 (Fig. 1A and 1B). Low power examination revealed that these
81 ductules were not randomly arranged. They outlined dimly
82 polygonal structures with terminal veins in the centers
83 and portal triads at the corners, that is, the classical hepatic
84 lobules. When micrographs of 40 serial sections stained
85 for cytokeratin-7 were digitally aligned and merged (Fig.
86 1C), this kind of perilobular arrangement of the ductules
87 was even more obvious. Two other characteristics could
88 be observed on this composite image: (i) no CK7+ biliary
89 ductules were present inside the hepatic lobules; (ii) the
90 ductules at the interlobular border spread until the half of
91 the porto-portal distances, which resulted in watershed-like
92 empty gaps in the middle of these stretches.

93 High power examination of individual biliary ductules
94 showed that these narrow tubules did really extend beyond
95 the limiting plate. The ductules spread in virtual "empty"
96 spaces among hepatocytes on cytokeratin antibody stained
97 sections (Fig. 1D), where only the epithelial elements of the
98 hepatic tissue were decorated. When the ductules terminated

99 on hepatocytes, they were surrounded by typical U-shaped
100 basement membrane (Fig. 2B inset), and the hepatocytes did
101 not participate in the composition of the ductules beyond
102 these connections. The "empty" space around the ductules
103 was filled by collagenous matrix (Fig. 2A) and contained
104 CD31+ small blood vessels (Fig. 2B), some of which were
105 also labeled by the arterial marker NG-2 [17] (Fig. 2C). Taken
106 together, confocal analysis of normal human liver revealed
107 the deposition of small amounts of extracellular matrix
108 between hepatic lobules, with expanding biliary ductules
109 and blood vessels. This kind of arrangement of the blood
110 vessels was described earlier as the vascular septum [18,19].
111 The small amount of matrix could not be visualized on tra-
112 ditional histological sections by special stainings on any of
113 our liver samples.

Alterations of the hepatic ductules with age

114 The maturation of the biliary system continues in post-
115 natal life in humans [20,21], and major changes are also
116 observed in rats [15,22]. Therefore, we decided to examine
117 the distribution of the canals of Hering in healthy livers of
118 individuals of various ages.

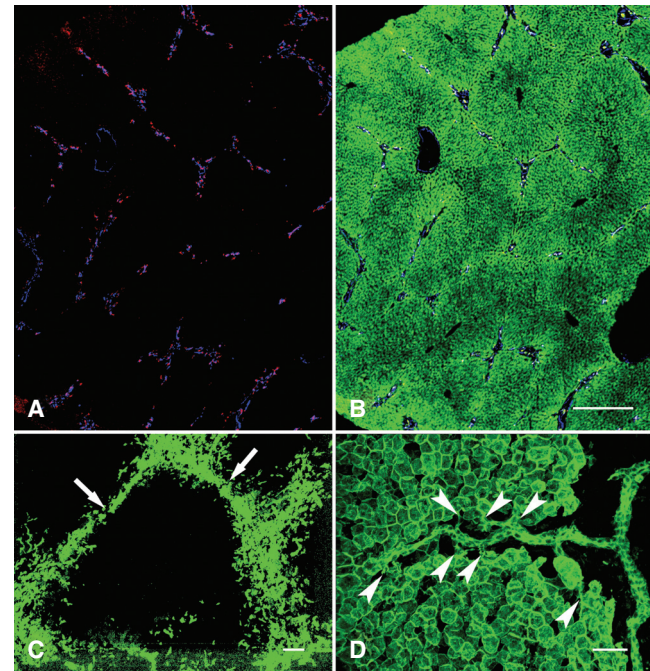


FIG. 1. Confocal images of normal human liver from a 3-year-old child. (A, B) Triple labeling for CK7 (red), laminin (blue), and pan CK (green). (A) CK7 (red) and laminin (blue) staining. (B) Merged image. Comparing the two images, the perilobular arrangement of the laminin-framed ductules is clearly discernible. (C) CK7 (green)-stained biliary ductules sharply outline the hepatic lobule when 40 thick serial sections are merged. Note the "gaps" (arrows) halfway of the porto-portal distances. (D) Horizontal view of 42 optical sections stained for panCK. Note the numerous connections of the bile ductules with the liver parenchyma (arrowheads). The collecting bile ductule is running in an "empty" space toward the portal area. Scale bar for A, B: 500 μm ; C: 100 μm ; and D: 50 μm .

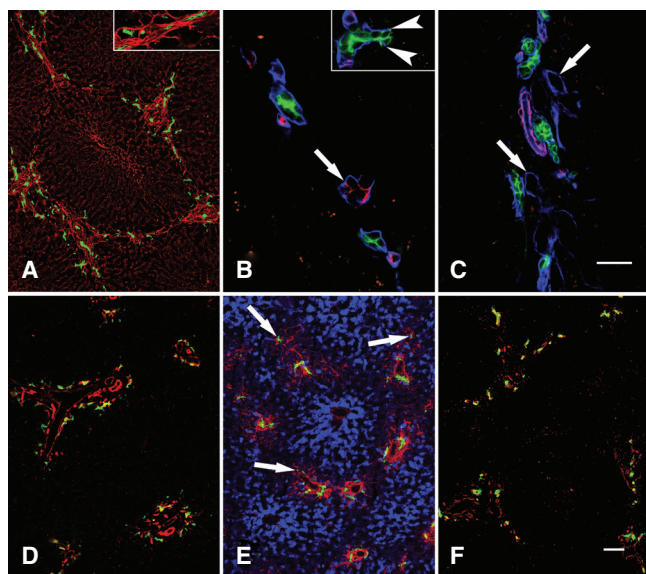


FIG. 2. Confocal images of normal human livers from a 3 (A, B)- and a 13 (C)-year-old child. (D–F) hepatic lobules in 23 (D)-, 39 (E)-week-old fetuses and in a 26-year-old adult (F) liver. (A) Double staining for CK7 and collagen I. CK7 (green)-stained perilobular ductules are embedded in rudimentary collagenous matrix (red) in the portal spaces and in the interlobular septa. The inset shows the vascular septum at a higher magnification on a different section. (B, C) High power view of the “vascular septum.” (B) Laminin (blue) surrounded CK7+ (green) ductules are accompanied by CD31 (red)-decorated blood vessels (arterioles). The larger vessel (arrow) probably represents a terminal branch of the portal vein. The inset shows the connection of a ductule on the hepatic plate (cannot be seen with this staining); note the sharp ending of the U-shaped basement membrane at the ducto-parenchymal border (arrowheads). (C) Note the proximity of NG-2+ (red) arterioles to the CK7 (green)-stained ductules. The empty laminin (blue) circles (arrows) probably represent portal vein branches. (D) The portal tracts are “closed”; laminin (red) surrounded CK7+ (green) ductules are confined to the border of the portal space. Note the high number of ductules marking the ductogenesis from the ductal plate. (E) Thy-1 (red)-stained myofibroblasts initiate the formation of the interlobular septa with a few CK7+ (green) ductules (arrows). The CYP450 (blue) staining shows the zonation of the hepatic lobule with a Thy-1-positive terminal vein in the center. (F) Laminin (red) and CK7 (green) marked ductules outline the hepatic lobule in the adult liver, but they are rarer in the septa than in children (compare with Fig. 1C, 1D). Scale bar for A, D, E, and F: 100 μ m and B and C: 50 μ m.

The portal areas in the liver of immature neonates born on the 23rd week of pregnancy were “closed.” There were numerous bile ducts in the periportal connective tissue, especially at the periphery, as the remnants of the ductal plate. However, no signs of vascular septa were seen; no matrix deposition, blood vessels, or biliary ductules could be observed outside the limiting plate in any of the examined specimens (Fig. 2D).

Early signs of vascular septum formation could already be recognized in a liver sample derived from a fetus of the

39th week of pregnancy. It was mostly outlined by Thy-1-positive myofibroblasts, but a few CK7+ ductules were also present in these septum fundamentals outside the portal fields (Fig. 2E).

The vascular septa and all of its components were mostly developed in the livers of young children of the age of 3 years (Fig. 1A and 1B). The only available liver specimen from a 13-year-old girl contained relatively regressed vascular septa, and although all the elements described earlier were present in the livers of young adults (20 and 26 years), they were more scarce (Fig. 2F).

Immunophenotypic characterization of bile ductules

There are several proposed markers for hepatic progenitor cells in human liver (1,2), but most of them did not distinguish hepatic ductules of the vascular septa from larger interlobular bile ducts in our hands. Some of the markers (AFP, chromogranin, synaptophysin, DMBT, DLK, CEA, CK20, CK14) did not label any biliary structures, while others (EpCAM, E-cadherin, CK7, CK19) stained the complete biliary tree (data not shown). Only three markers reacted differentially with bile ducts and ductules. Epithelial membrane antigen (EMA) resulted in a very sharp characteristic linear apical staining in the interlobular bile ducts. Conversely, it was absent in the ductules even on cross sections (Fig. 3A and 3B). The staining pattern of CD133 (Fig. 3C) and CD56 (Fig. 3D, 3E, and 3F) was opposite. In specimens up to the age of 3 years, there was a consistent apical CD133 staining in all segments of the biliary tree. However, in samples from older individuals the staining was strictly confined to the small ductules of the vascular septa. The distribution of CD56 in all specimens was similar to this latter case: it labeled exclusively the small ductules.

Quantitative evaluation of the immunohistochemical reactions (Table 1) showed that only a small portion of the biliary structures were stained for EMA, and this staining was restricted to the periportal area. No such preferential distribution was noticed with the two other markers. Almost all ducts/ductules were decorated by CD133 in the livers of the children, while in adulthood the ratio of CD56+ and CD133+ ductules were similar. The CK7 antibody reacted sometimes with very small bile ductules occasionally appearing as single cells especially along the vascular septa. Since the CD56 and CD133 reaction was not as strong and diffuse as the CK7, the number of the CD56 and CD133 ductules was probably underestimated.

Discussion

We have analyzed the architecture of biliary ductules in normal human livers and observed them to circumscribe the classical hepatic lobules by participating in the formation of the so-called vascular septa (Fig. 4). This arrangement develops in postnatal life and can be most obviously seen in early childhood. The hepatic ductules are characterized by a unique EMA-/CD56+/CD133+ immunophenotype.

There are several candidates for the liver stem/progenitor cell niche. Kuwahara et al. [10] proposed four structures to harbor such cells: the canals of Hering, intralobular bile ducts, periductal “null” mononuclear cells, and peribiliary hepatocytes. After all, stemness has been proposed to be not an entity but function [23] and—depending on the

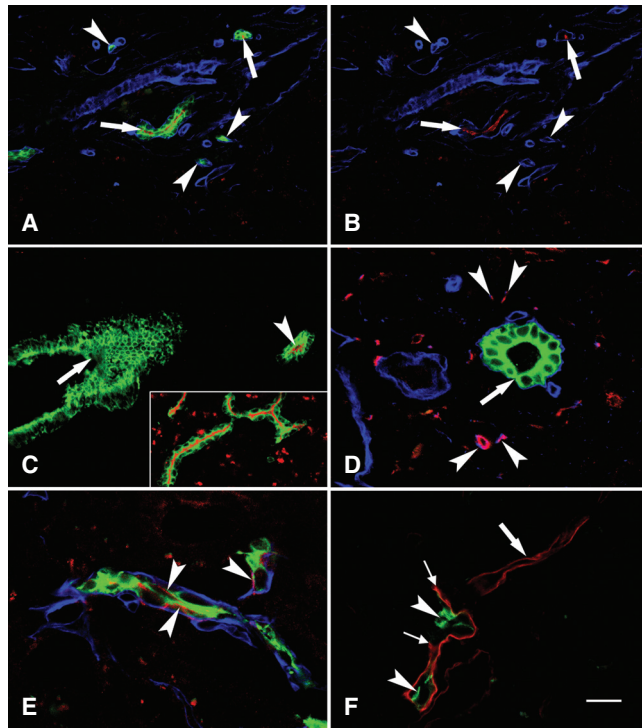


FIG. 3. Immunophenotypical characterization of the hepatic ductules in adult (A–C) and 3-year-old (D–F) livers. (A, B) There is a sharp apical epithelial membrane antigen (EMA) (red) staining in CK7 (green)- and laminin (blue)-marked bile ducts (arrows) inside the portal space, while EMA staining is absent in the small ductules (arrowheads) at the periphery. For better visibility of the EMA staining B shows only the red and blue channels. (C) There is an apical CD133 (red) staining in a CK7 (green)-marked ductule (arrowhead), while this marker is not present in an interlobular bile duct (arrow). The inset shows the apical CD133 positivity of ductules. (D) CD56 (red) stains only the small nerves (arrowheads) in the portal space, the CK7 (green)- and laminin (blue)-labeled bile duct is negative (arrow). (E) High magnification of a CK7 (green)- and laminin (blue)-stained ductule within the septum reveals membranous CD56 (red) positivity (arrowheads). (F) CD56+ (green) bile ductules (arrowheads) are attached to hepatocytes (not highlighted by this staining), are surrounded by laminin-positive (red) U-shaped basement membrane (small arrows). The laminin (red)-positive “empty” structure surrounded by basement membrane (large arrow) represents a blood vessel. Scale bar: 50 μ m.

186 situation—different cell populations can behave as hepatic
187 progenitor cells. Insofar, most evidence shows that the canals
188 of Hering have the highest potential to behave as hepatic
189 progenitor cells [1,2,6,13]. Therefore, the accurate architecte-
190 ture of these structures is a key issue to understand their
191 behavior under normal and pathological conditions.

192 The canals of Hering were originally described [11] as
193 short straight ducts at the limiting plate, which connect
194 the bile canaliculi to the interlobular bile ducts. However,
195 Theise et al. [16] demonstrated the extension of hepatic
196 ductules through the limiting plate into the hepatic lobule.
197 Our results confirm the presence of these structures deep

TABLE 1. IMMUNOPHENOTYPE OF BILIARY STRUCTURES
IN NORMAL LIVER

Sample	CK7+	EMA+	CD56+	CD133+
3 years	100% (1,112)	4.8%	62.9%	96.3%
Adult	100% (1,125)	6.7%	54.4%	59%

Abbreviation: EMA, epithelial membrane antigen.

() Total number of counted bile ducts.

in the hepatic parenchyma; moreover, a clear orientation of
the ductules could be observed on our confocal images. The
ductules spread into the parenchyma along the porto-portal
axis. The hexagonal structures outlined by hepatic ductules
correspond to the classical hepatic lobules. High power
examination of individual ductules revealed their close cor-
relation with bile canaliculi enabling their drainage.

In addition to former observations [19,24] that venular
branches are present in vascular septa, we noticed NG-2-
stained arterioles running in line with the ductules. There
have been speculations about bile ductule escorting hepatic
arterioles [18,19,25,26,27] but no convincing evidence has
been published so far. Gouw et al. [19] and van der Heuvel
et al. [28] emphasize the importance of the microvascu-
lar compartment for the efficient regeneration of ductules.
Since—contrary to several other species—no arterio-portal
anastomoses exist in the human liver, the presence of arte-
rial blood would be advantageous for the regenerative func-
tion of the ductules. The proximity of the blood vessels to the
bile ductules corresponds very well to the close correlation
between the development of biliary and vascular structures
[29]. This architecture of the intraparenchymal ductules and
the escorting vessels is in full agreement with the proposed
model of Matsumoto [18] based on 3D reconstruction of the
human liver from thousands of serial sections.

According to the original description [18], the “vascu-
lar septum” is not a fibrous septum but a vascular surface
from which sinusoids originate. However, we observed a
collagenous matrix in this location. Since all the studied
liver samples were normal and no fibrosis could be seen
by traditional connective tissue staining, we suggest that a
minimal amount of matrix material in the vascular septum,
which can be visualized only by careful immunohistochem-
ical analysis, is a component of the normal human hepatic
tissue. Hepatic lobules are separated by well-defined con-
nective tissue septa in several species [30], and the vascular
septum of the human liver with its matrix components can
be regarded as a rudimentary interlobular septum.

We have observed a peculiar age dependence of the vas-
cular septa. Obviously, a more detailed age-related analysis
of these structures is required. The interlobular bile ducts
develop from the ductal plate [21], but ductal plates disap-
pear shortly after birth and new bile ducts/ductules arise
from pre-existent ducts by branching and elongation [31].
This “cholangiogenesis” could follow the primitive septa we
observed in the liver of the 39-week-old fetus. The postnatal
maturation of the biliary tree is well documented in humans
[21] and rats [22] as well. Furthermore, the interlobular sep-
tum also develops postnatally in pigs [30].

The progressing scarcity of the ductular system with age
should also be analyzed in more detail. We do not know if
this process is absolute due to the apoptosis of biliary cells or

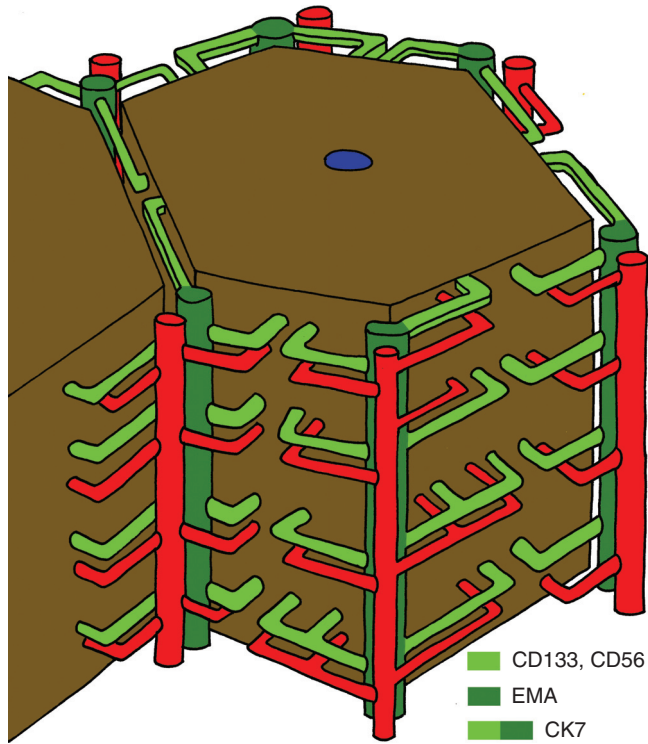


FIG. 4. Schematic representation of hepatic lobule (brown), with bile ducts/ductules (green) and accompanying arterioles (red). Note that these structures extend only halfway into the porto-portal distances; however, they cover the whole “lateral” surface of the lobule. For simplicity, the portal vein branches are not shown.

250 just relative. The size of the hepatic lobules increases during
251 ontogeny [32], and if the growth of the ductules is arrested
252 earlier, it may be responsible for their relative regression.

253 We were curious if the biliary ductules could be char-
254 acterized by a special immunophenotype. Three different
255 antibodies were able to distinguish reliably the canals of
256 Hering from larger bile ducts: the canals of Hering were
257 EMA⁻/CD56⁺/CD133⁺; whereas, interlobular bile ducts
258 were EMA⁺/CD56⁻/CD133⁻. All of these markers have
259 already been mentioned in connection with the hepatic pro-
260 genitor cell compartment. Atypical ductular reactions have
261 been reported EMA⁻/CD56⁺, while the typical ones, which
262 are similar to the interlobular bile ducts, are EMA⁺/CD56⁻
263 [33]. CD56 has been demonstrated in proliferating ductules,
264 while it could not be observed in normal canals of Hering
265 [34,35], but recent studies found CD56 mRNA and protein
266 in ductules of normal human livers [36,37]. CD133 has origi-
267 nally been described as a hematopoietic stem cell marker,
268 and its mRNA has been detected in the liver by Northern
269 hybridization, but no immunostaining was identified in par-
270 affin sections by Miraglia et al. [38]. However, the protein
271 could be detected by immunohistochemistry in the canals of
272 Hering of normal human liver [39] and in regenerating
273 ductules related to fulminant liver failure [40]. In our present
274 experiments, the distribution of this marker showed an age-
275 dependent change. This is similar to our results on rat liver,
276 where the immunophenotype of the canals of Hering devel-
277 oped postnatally [15]. Interestingly, CD133⁺ cells isolated

from HCC proved to be highly tumorigenic and have been
278 reported as tumor stem cells [41]. Increased expression of
279 CD133 has also been reported in a subset of cholangiocel-
280 lular carcinomas, which were claimed to have a progenitor
281 cell origin [42].

The combined application of these three antibodies pro-
283 vides an efficient tool for the identification of the canals of
284 Hering in the normal human liver. Furthermore, the distinct
285 immunophenotype of the hepatic ductules supports their
286 different biological potential.

In conclusion, we present a refinement for the widely
288 cited architectural description [16,27,43] of the intraparen-
289 chymal biliary ductules in normal human liver. The canals
290 of Hering with escorting vessels are situated in the vascular
291 septum and are components of a rudimentary interlobular
292 septum. They can be distinguished from larger bile ducts
293 by a unique immunophenotype. Better comprehension of
294 canals of Hering’s architecture in normal human liver may
295 promote our understanding of their behavior in various
296 pathological/biological reactions.

Acknowledgment

The authors appreciate the help of Dr. Nóra Szlávik, Dr.
298 Éva Görbe, and Dr. Júlia Hajdú in collecting the samples.
299 The article is supported by OTKA K 67697.
300

Author Disclosure Statement

We declare that we have no duality of interest.

References

1. Alison MR, P Vig, F Russo, BW Bigger, E Amofah, M Themis and S Forbes. (2004). Hepatic stem cells: from inside and outside the liver? *Cell Prolif* 37:1–21. 302
2. Santoni-Rugiu E, P Jelnes, SS Thorgeirsson and HC Bisgaard. (2005). Progenitor cells in liver regeneration: molecular responses controlling their activation and expansion. *APMIS* 113:876–902. 303
3. Dahlke MH, FC Popp, S Larsen, HJ Schlitt and JEJ Rasko. (2004). Stem cell therapy of the liver-fusion or fiction? *Liver Transpl* 10:471–479. 304
4. Tosh D and A Strain. (2005). Liver stem cells-prospects for clinical use. *J Hepatol* 42:S75–S84. 305
5. Thorgeirsson SS and JW Grisham. (2006). Hematopoietic cells as hepatocyte stem cells: a critical review of the evidence. *Hepatology* 43:2–8. 306
6. Fausto N. (2004). Liver regeneration and repair: hepatocytes, progenitor cells, and stem cells. *Hepatology* 39:1477–1487. 307
7. Grompe M. (2003). The role of bone marrow stem cells in liver regeneration. *Semin Liver Dis* 23:363–371. 308
8. Fujita M, H Furukawa, M Hattori, S Todo, Y Ishida and K Nagashima. (2000). Sequential observation of liver cell regeneration after massive hepatic necrosis in auxiliary partial orthotopic liver transplantation. *Mod Pathol* 13:152–157. 309
9. Eleazar JA, L Memeo, JS Jhang, MM Mansukhani, S Chin, SM Park, JH Lefkowitz and G Bhagat. (2004). Progenitor cell expansion: an important source of hepatocyte regeneration in chronic hepatitis. *J Hepatol* 41:983–991. 310
10. Kuwahara R, AV Kofman, CS Landis, ES Swenson, E Barendswaard and ND Theise. (2008). The hepatic stem cell niche: identification by label-retaining cell assay. *Hepatology* 47:1994–2002. 311
11. Hering E. (1867). Über den Bau der Wirbelthierleber. *Arch Mikrosk Anat* 3:88–114. 312

- 335 12. Grisham JW and EA Porta. (1964). Origin and fate of proliferated hepatic ductal cells in rat: electron microscopic and autoradiographic studies. *Exp Mol Pathol* 3:242–261. 399
- 336 13. Paku S, J Schnur, P Nagy and SS Thorgeirsson. (2001). Origin and structural evolution of the early proliferating oval cells in rat liver. *Am J Pathol* 158:1313–1323. 400
- 337 14. Scheres B. (2007). Stem-cell niches: nursery rhymes across kingdoms. *Nature Rev Mol Cell Biol* 8:345–354. 401
- 338 15. Paku S, K Dezső, L Kopper and P Nagy. (2005). Immunohistochemical analysis of cytokeratin 7 expression in resting and proliferating biliary structures of rat liver. *Hepatology* 42:863–870. 402
- 339 16. Theise ND, R Saxena, BC Portmann, SN Thung, H Yee, L Chiriboga, A Kumar and JM Crawford. (1999). The canals of Hering and hepatic stem cells in humans. *Hepatology* 30:1425–1433. 403
- 340 17. Fukushi J, IT Makagiansar and WB Stallcup. (2004). NG2 proteoglycan promotes endothelial cell motility and angiogenesis via engagement of Galectin-3 and $\alpha 3 \beta 1$ integrin. *Mol Biol Cell* 15:3580–3590. 404
- 341 18. Matsumoto T, R Komori, T Magara, T Ui, M Kawakami, T Tokuda, S Takasaki, H Hayashi, K Jo, H Hano and H Tanaka. (1979). A study on the normal structure of the human liver, with special reference to its angioarchitecture. *Jikeikai Med J* 26:1–40. 405
- 342 19. Gouw AS, MC van der Heuvel, M Boot, MJ Slooff, S Poppema and KP de Jong. (2006). Dynamics of the vascular profile of the finer ranches of the biliary tree in normal ad diseased human livers. *J Hepatol* 45:393–400. 406
- 343 20. Crawford JM. (2002). Development of the intrahepatic biliary tree. *Semin Liver Dis* 22:213–226. 407
- 344 21. Lemaigre FP. (2003). Development of the biliary tract. *Mech Dev* 120:81–87. 408
- 345 22. Van Eyken P, R Sciote and V Desmet. (1988). Intrahepatic bile duct development in the rat. *Lab Invest* 59:52–59. 409
- 346 23. Blau HM, TR Brazelton and JM Weimann. (2001). The evolving concept of a stem cell: entity or function? *Cell* 105:829–841. 410
- 347 24. Teutsch HF. (2005). The modular microarchitecture of human liver. *Hepatology* 42:317–325. 411
- 348 25. Yamamoto K, I Sherman, MJ Phillips and MM Fisher. (1985). Three-dimensional observations of the hepatic arterial terminations in rat, hamster and human liver by scanning electron microscopy of microvascular casts. *Hepatology* 5:452–456. 412
- 349 26. RNM MacSween, VJ Desmet, T Roskams and RJ Scotthorne. (2002). Developmental anatomy and normal structure. In: *Pathology of the Liver*. MacSween RNM, AD Burt, BC Portmann, KG Ishak, PJ Scheuer, PP Anthony, eds. Churchill Livingstone, London, pp 1–66. 413
- 350 27. Saxena R, ND Theise and JM Crawford. (1999). Microanatomy of the human liver-exploring the hidden interfaces. *Hepatology* 30:1339–1346. 414
- 351 28. Van der Heuvel MC, KP de Jong, M Boot, MJ Sloff, S Poppema and AS Gouw. (2006). Preservation of bile ductules mitigates bile duct loss. *Am J Transplant* 6:2660–2671. 415
- 352 29. Libbrecht L, D Cassiman and V Desmet. (2002). The correlation between portal myofibroblasts and development of intrahepatic bile ducts and arterial branches in human liver. *Liver* 22:252–258. 416
- 353 30. Ekataksin W and K Wake. (1997). New concepts in biliary and vascular anatomy of the liver. *Prog Liver Dis* 15:1–30. 417
- 354 31. Roskams T and V Desmet. (2008). Embryology of extra- and intrahepatic bile ducts, the ductal plate. *Anat Rec* 291:628–635. 418
- 355 32. PappV, K Dezső, V László, P Nagy and S Paku. (2009). Architectural changes during regenerative and ontogenic liver growth in the rat. *Liver Transplant* 15:177–183. 419
- 356 33. Sonzogni A, G Colloredo, L Fabris, M Cadamuro, B Paris, L Roffi, M Pozzi, G Bovo, P Del Poggio, BC Portmann and M Strazzabosco. (2004). Isolated idiopathic bile ductular hyperplasia in patients with persistently abnormal liver function tests. *J Hepatol* 40:592–598. 420
- 357 34. Van der Heuvel MC, MJH Slooff, L Visser, M Muller, KP DeJong, S Poppema and AS Gouw. (2001). Expression of anti-OV6 antibody and anti-N-CAM antibody along the biliary line of normal and diseased human livers. *Hepatology* 33:1387–1393. 421
- 358 35. Zhou H, LE Rogler, L Teperman, G Morgan and CE Rogler. (2007). Identification of hepatocytic and bile ductular cell lineages and candidate stem cells in bipolar ductular reactions in cirrhotic human liver. *Hepatology* 45:716–724. 422
- 359 36. Schmelzer E, E Wauthier and LM Reid. (2006). The phenotypes of pluripotent human hepatic progenitors. *Stem Cells* 24:1852–1858. 423
- 360 37. Zhang L, N Theise, M Chua and LM Reid. (2008). The stem cell niche of human livers. *Hepatology* 48:1598–1607. 424
- 361 38. Miraglia S, W Godfrey and AH Yin. (1997). A novel five-transmembrane hematopoietic stem cell antigen: isolation, characterization, and molecular cloning. *Blood* 90:5013–5021. 425
- 362 39. Karbanová J, E Missol-Kolka, A Fonseca, C Lorra, P Janich, H Hollerová, J Jászai, J Ehrmann, Z Kolar, C Liebers, S Arl, D Subrtová, D Freund, J Mokry, WB Huttner and D Corbelli. (2008). The stem cell marker CD 133 (Prominin-1) is expressed in various human glandular epithelia. *J Histochem Cytochem* 56:977–993. 426
- 363 40. Craig CEH, A Quaglia, C Selden, M Lowdell, H Hodgson and AP Dhillon. (2004). The histopathology of regeneration in massive hepatic necrosis. *Semin Liver Dis* 24:49–64. 427
- 364 41. Ma S, K Chan, L Hu, TK Lee, JY Wo, IO Ng, BJ Zheng and XY Guan. (2007). Identification and characterization of tumorigenic liver cancer stem/progenitor cells. *Gastroenterology* 132:2542–2556. 428
- 365 42. Komuta M, B Spee, SV Borghot, R De Vos, C Verslype, R Aerts, H Yano, T Suzuki, M Matsuda, H Fujii, V Desmet, M Kojiro and T Roskams. (2008). Clinicopathological study on cholangiolocellular carcinoma suggesting hepatic progenitor cell origin. *Hepatology* 47:1544–1556. 429
- 366 43. Roskams TA, ND Theise, C Balabaud, G Bhagat, PS Bhathal, P Bioulac-Sage, EM Brunt, JM Crawford, HA Crosby, V Desmet, MJ Finegold, SA Geller, AS Gouw, P Hytiroglou, AS Knisely, M Kojiro, JH Lefkowitz, Y Nakanuma, JK Olynyk, YN Park, B Portmann, R Saxena, PJ Scheuer, AJ Strain, SN Thung, IR Wanless and AB West. (2004). Nomenclature of the finer branches of the biliary tree: canals, ductules, and ductular reactions in human livers. *Hepatology* 39:1739–1745. 430

Address correspondence to:

Dr. Peter Nagy
 First Department of Pathology and
 Experimental Cancer Research
 Semmelweis University
 Üllői út 26
 Budapest 1085
 Hungary

E-mail: nagy@korb1.sote.hu

Received for publication April 1, 2009

Accepted after revision June 24, 2009

SUPPLEMENTARY TABLE 1. PRIMARY ANTIBODIES USED FOR THE IMMUNOHISTOCHEMICAL STUDIES

<i>Antibody</i>	<i>Species</i>	<i>Manufacturer</i>	<i>Catalog number</i>	<i>Dilution</i>
Laminin	Rabbit polyclonal	Dako	Z0097	1:200
FITC-labeled pancytokeratin	Mouse monoclonal	Dako	F0859	1:20
FITC-labeled cytokeratin-7	Mouse monoclonal	Dako	F7232	1:10
Cytokeratin-7	Mouse monoclonal	BioGenex	MU-255-UC	1:50
CD31	Mouse monoclonal	Dako	M0823	1:50
NG-2	Mouse monoclonal	R&D	MAB2585	1:20
Thy-1	Mouse monoclonal	BD Pharmingen	550402	1:100
Cyp450 IIE1	Rabbit polyclonal	MBL	BV-3084-3	1:100
EMA	Mouse monoclonal	Novocastra	EMA-L-CE	1:50
CD56	Mouse monoclonal	BD Pharmingen	559043	1:50
CD133	Mouse monoclonal	Miltenyi Biotec	120-000-967	1:50
Collagen I	Rabbit polyclonal	Calbiochem	234167	1:50

Abbreviation: EMA, epithelial membrane antigen.